The Journal of Neuroscience, February 1994, 14(2): 796–808

Extension of Synaptic Extracellular Matrix During Nerve Terminal Sprouting in Living Frog Neuromuscular Junctions

Lanlin Chen and Chien-Ping Ko

Department of Biological Sciences, Section of Neurobiology, University of Southern California, Los Angeles, California 90089-2520

Remodeling of the synaptic extracellular matrix (ECM) and its dynamic relationship with nerve terminal plasticity have been demonstrated in normal frog neuromuscular junctions (NMJs) *in vivo* (Chen et al., 1991). Our previous work has led to a hypothesis that extension of synaptic ECM precedes nerve terminal growth during synaptic remodeling. To test this hypothesis, the present study examined the changes of synaptic ECM in frog NMJs that were primarily undergoing nerve terminal growth and sprouting. Frog sartorius muscles were double stained with a fluorescent nerve terminal dye (4-Di-2-Asp) and rhodamine-tagged peanut agglutinin (PNA), which recognizes synaptic ECM. The double-labeled NMJs were visualized *in vivo* with video-enhanced fluorescence microscopy. Nerve sprouting was then induced in the muscle by grafting segments of the contralateral sciatic nerve. The identified NMJs were restrained and reexamined 2–3 months later. Extensive sprouting was observed in 46% of 167 identified NMJs. At junctional regions that showed extension or formation of new branches, synaptic ECM was commonly seen to have the same shape and distribution as the nerve terminal. However, extension of synaptic ECM beyond the corresponding nerve terminals, often by tens of microns, was observed in 29% of these newly formed junctional regions. This lack of correlation might be transient, as growth of nerve terminals following extended, PNA-stained ECM was seen. Examination with histological staining not only confirmed a lack of nerve terminal at the extended synaptic ECM region but also indicated an absence of AChE and postsynaptic junctional folds. The absence of these postsynaptic specializations at the extended, PNA-stained ECM region makes it unlikely that this region was previously occupied by nerve terminals that had retracted. Thus, the present study provides further findings consistent with the hypothesis that synaptic ECM precedes nerve terminal outgrowth and that the extension of synaptic ECM may play a role in synaptic remodeling.

[Key words: extracellular matrix, neuromuscular junction, peanut agglutinin, nerve sprouting, synaptic remodeling, video-enhanced microscopy]

Structural remodeling of synaptic connections has been observed in a variety of adult nervous tissues using conventional histology (reviewed by Wernig and Herrera, 1986) and, more recently, repeated *in vivo* imaging techniques (reviewed by Purves, 1989). Due to its accessibility and simplicity, the neuromuscular junction (NMJ) has been a particularly useful model system for studying the dynamic properties of the synapse. By repeatedly viewing the same NMJ at multiple times in living animals, varying degrees of synaptic remodeling have been observed in muscles with different fiber types and in muscles of different species. For example, NMJs in mouse fast-twitch muscle show proportionate expansion of existing junctional branches without a change in the number or pattern of branches (Lichtman et al., 1987; Balice-Gordon and Lichtman, 1990), whereas NMJs in slow-twitch muscle exhibit small disproportionate changes (Wigston, 1989, 1990) and filopodia of 1–2 μm in length (Robbins and Polak, 1988). In comparison, frog NMJs undergo dramatic remodeling, including growth, retraction, formation of new branches, and deletion of old ones, in a matter of months (Herrera and Werle, 1990; Herrera et al., 1990; Chen et al., 1991; Ko, 1991). However, the cellular and molecular mechanisms of synaptic remodeling remain unknown.

The extracellular matrix (ECM) is thought to be involved in the regulation of neural development, including axonal growth and synapse formation (for reviews, see Sanes, 1983, 1989; Reichardt and Tomaselli, 1991). In order to learn the possible role of synaptic ECM in the remodeling and maintenance of mature NMJs, we have previously examined the remodeling of synaptic ECM and its dynamic relationship with nerve terminals in living adult frog NMJs (Chen et al., 1991). By double labeling NMJs with a fluorescent nerve terminal dye, 4-Di-2-Asp (Magrassi et al., 1987), and rhodamine-conjugated peanut agglutinin (PNA) for the synaptic ECM (Ko, 1987, 1991), we have shown extensive remodeling not only in nerve terminals, but also in synaptic ECM. Although the close apposition between the nerve terminal and synaptic ECM at NMJs is, in general, actively maintained throughout the adult life, a lack of correlation between these two synaptic components was also observed. For example, along with the elongation or formation of new nerve terminal branches, synaptic ECM was sometimes seen extending tens of microns beyond nerve endings. The results led us to propose a hypothesis that the extension of synaptic ECM occurs prior to outgrowth of the nerve terminal during synaptic remodeling and may play a role in the dynamic feature of synaptic connections (Chen et al., 1991; Ko, 1991).

The present study aimed to test this hypothesis by examining the extension of synaptic ECM during nerve terminal sprouting

Received June 23, 1993; accepted Aug. 4, 1993.

This work was supported by NIH Grant NS 17954. We thank Drs. S. H. Astrow, W. L. Byerly, A. A. Herrera, and D. Morgan for critical comments on the manuscript.

Correspondence should be addressed to Dr. Chien-Ping Ko at the above address.

in living frog NMJs. Two approaches, in addition to those used in our previous work, were applied to this study. First, nerve terminal sprouting was induced by grafting nerve segments to the sartorius muscle to enhance nerve terminal growth (Diaz and Pecot-Dechavassine, 1990). This approach allows us to examine whether the extension of synaptic ECM precedes nerve terminal sprouts in the NMJs that are primarily undergoing extension. In our previous study on normal muscles (Chen et al., 1991), only about 10% of NMJs displayed a mismatch between the nerve terminal and synaptic ECM, and some of these junctions were undergoing retraction of nerve terminal branches. Thus, by examining synaptic remodeling during enhanced growth of nerve terminal sprouting, we expect to find more NMJs with synaptic ECM longer than nerve terminals. The increase in these types of NMJs would provide more examples to characterize further the nature of synaptic remodeling in adult synapses. The second approach was to combine the repeated *in vivo* observations with histological methods for staining nerve terminals and postsynaptic AChE at the final observations. The histological staining would help to confirm the absence of nerve terminal at the extended synaptic ECM region as observed by the 4-Di-2-Asp staining. In addition, the combined staining for nerve terminals and AChE would allow us to further distinguish growing synapses from regressing ones, as has been done by Wernig et al. (1980).

Consistent with our hypothesis, the present study has shown more NMJs (65% compared with 10% in controls) with extension of synaptic ECM longer than nerve terminals in the muscles in which sprouting was induced. Neither the fluorescent dyes nor the histological staining for nerve terminals revealed any nerve endings at the extended synaptic ECM regions. In addition, the absence of postsynaptic specializations, such as AChE reaction product and junctional folds, at the extended synaptic ECM regions suggests that they are newly differentiated regions rather than abandoned junctional sites. The results provide further evidence that the synaptic ECM recognized by PNA precedes the outgrowth of nerve terminals during the remodeling of NMJs.

A preliminary report of these results has been presented (Chen and Ko, 1991).

Materials and Methods

Animal preparation. Adult male and female frogs (*Rana pipiens*) of similar size (7–8 cm, rump-to-nose length) and weight (30–41 gm) were used for all the experiments. These frogs were obtained all year round and maintained in the laboratory from several weeks to 2–3 months before experiments. Animals were anesthetized by immersion in 0.2% tricaine methanesulfonate (Sigma) for approximately 30 min and then kept on ice to maintain a low body temperature throughout the surgery and staining. The details of the double-staining procedure, using a fluorescent dye, 4-(4-diethylamino-styryl)-*N*-methylpyridinium iodide (4-Di-2-Asp; Molecular Probe), for nerve terminals (Magrassi et al., 1987) and tetramethylrhodamine isothiocyanate–conjugated peanut agglutinin (TMR-PNA; Sigma) for the synaptic ECM (Ko, 1987), have been described in a previous report (Chen et al., 1991). Briefly, an incision (2–3 cm length) was made on the right leg to expose sartorius muscle. A strip of Kimwipe tissue, moistened with frog Ringer solution (111 mM NaCl, 2 mM KCl, 1.8 mM $CaCl_2$, 5 mM HEPES, pH 7.2), was placed on the muscle surface. The 4-Di-2-Asp staining solution (10 μM in Ringer solution) was dripped with a pipette onto the strip of Kimwipe tissue every 30 sec, for a total of 3 min. The sartorius muscle was rinsed with frog Ringer and then stained by the same method with TMR-PNA (50 μg/ml in Ringer solution) for a total of 30 min, with 3–4 min between each application. After staining, the Kimwipe tissue was removed and the muscle rinsed several times with frog Ringer solution. The frog was then placed on a metal plate connected to a recirculating chiller that kept the temperature of the plate at 0–4°C. The metal plate was attached to the stage of an epifluorescence microscope (Olympus BH2-RFL), allowing visualization of the fluorescently stained NMJs.

Visualization of NMJs and image processing. The method for visualization of NMJs and image processing has been explained in detail in the previous report (Chen et al., 1991). The nerve entry position, used as a landmark, was first located with a 10× objective and oblique incident illumination from a fiber optic light. NMJs are commonly distributed along intramuscular nerve bundles found near the nerve entry forming several junctional regions. By using epifluorescence optics for TMR-PNA, the approximate distance of each junctional region to the point of nerve entry or the distance between each junctional region was quickly estimated. The individual NMJs in each junctional region were then viewed with a 50× water-immersion objective (Leitz; NA 1.0) and the image recorded using a low-light video camera (Dage, SIT 66). Filters (Olympus BP490/EY475, G520) for blue excitation/green emission were used to visualize 4-Di-2-Asp–stained nerve terminals and green excitation/red emission filters (Olympus BP545/EY550, R610) were used for TMR-PNA–stained ECM. To avoid excessive illumination, a 1.2% transmittance neutral density filter was used to attenuate the light source (100 W Hg) and the exposure time for viewing both fluorescent labels was kept less than 20 sec. The recorded images through SIT camera were further processed using a digital image processor (Image-1, Universal Imaging). Images (64 video frames) were averaged and then processed to reduce background and enhance contrast. The processed images were then stored on videotape and/or computer diskettes and later photographed using 35 mm films or a video printer.

Two to three months following nerve implantation surgery (see below), the right sartorius muscle was restained with 4-Di-2-Asp and TMR-PNA and identified NMJs were viewed for the second time. Some NMJs were viewed a third time about 10–15 d after the second observation. Reidentification of the NMJ was based on the fluorescent images obtained during the initial observation and the location of the NMJ from the nerve entry position, as well as the distance from each other. The subsequent viewing procedures and image processing were the same as described above.

Nerve segment implantation. To induce axonal sprouting, the technique of nerve implantation, similar to that described by Diaz and Pecot-Dechavassine (1990), was adopted. Following the initial visualization of identified NMJs in the right sartorius muscle as described above, peripheral nerve segments were implanted under the muscle. Two small incisions were made along the medial edge of the right sartorius muscle, near the pelvis and nerve entry, respectively, and the muscle at these two sites was gently lifted free from the adjacent muscles using a glass probe. Two segments of the contralateral sciatic nerve, 2–3 mm each, were removed and placed separately at each location in the right sartorius muscle. Nerve segments were positioned parallel to the long axis of muscle fibers close to the middle of the muscle. The skin was then sutured closed and the frog was returned to its tank for recovery.

Histology. After the final *in vivo* observation, the right sartorius muscle was dissected out and fixed with 2% glutaraldehyde (in frog Ringer solution) for 3–4 min (pH 7.2). The muscle was then stained with nitroblue tetrazolium (NBT) for nerve terminals (Letinsky and DeCino, 1980) and Karnovsky's method for acetylcholinesterase (AChE) (Karnovsky, 1964). The histological images of NMJs were compared with the final fluorescent images of the same junction. Some muscles were stained with horseradish peroxidase–conjugated PNA (HRP-PNA) instead of NBT/AChE staining after the final *in vivo* observation. For HRP-PNA staining, muscles were fixed overnight with 2% glutaraldehyde at 4°C. After incubation with HRP-PNA (100 μg/ml in Ringer solution; Sigma) at room temperature for 1 hr or at 4°C overnight, muscles were rinsed with Ringer solution thoroughly and subjected to the peroxidase enzyme reaction using a peroxidase substrate kit (Vector).

NMJs double stained with fluorescently labeled PNA and tetanus toxin C-fragment. Some sartorius muscles were dissected from normal frogs and double stained with TMR-PNA and fluorescein isothiocyanate–tagged tetanus toxin C-fragment (TTC), which has been shown to label nerve membrane (Robbins and Polak, 1988). A strip of Kimwipe tissue soaked in 10–20 μl of TTC solution (100 μg/ml in Ringer; Molecular Probe) was placed on the surface of the muscle. The dish was then covered and sealed with paraffin film to prevent evaporation. After 30–45 min of staining, the muscle was rinsed thoroughly with Ringer and incubated with TMR-PNA (50 μg/ml in Ringer) for 30 min. After double labeling, NMJs were observed with the epifluorescence microscope.

Measurements. To quantify the changes following nerve implantation

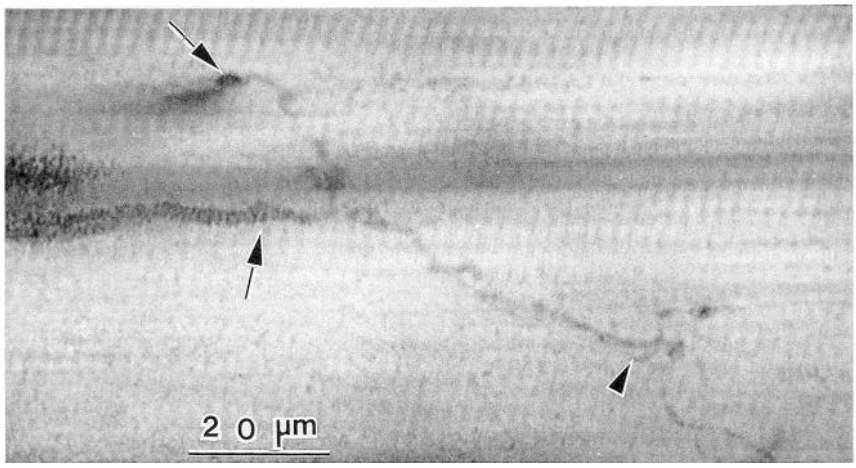

Figure 1. An NMJ undergoing sprouting after implantation of sciatic nerve segments to the frog sartorius muscle (see Materials and Methods). The end plate was stained with NBT and Karnovsky's method to reveal the nerve terminal arborization and postsynaptic AChE 76 d after operation. The thin nerve fibers (*arrowhead*) extended past the border of the AChE staining (*lower arrow*). The *upper arrow* indicates a ring of AChE staining at the end of a sprout.

in both nerve terminals and synaptic ECM, the fluorescent images of 4-Di-2-Asp and TMR-PNA staining were traced from a video monitor onto acetate film and measurements were then made on a digitizing tablet connected to a computer (Chen et al., 1991). The frequency and extent of nerve sprouting were determined based on images of NBT and Karnovsky's staining. A nerve sprout was identified either as a "naked" nerve process without accompanying AChE, or with AChE ring-like structure (Wernig et al., 1980). The difference in length between 4-Di-2-Asp staining and TMR-PNA staining at each sprouting branch (identified by the NBT/AChE staining) was also calculated. Because PNA staining of synaptic ECM is not as sharply defined as nerve terminal staining, the tracing of PNA staining from the video monitor occupied about 3–4 μm in width. Thus, only the difference equal to or more than 5 μm between nerve terminal and PNA staining was analyzed.

Results

Induction of nerve sprouting in sartorius muscles

Similar to the previous findings (Diaz and Pecot-Dechavassine, 1990; Pecot-Dechavassine and Diaz, 1991), extensive nerve sprouting in the sartorius muscle occurred around 2–3 months after nerve implantation. Thus, the subsequent observations of identified NMJs were usually made around this period. When NMJs were stained with the NBT technique for nerve terminals and Karnovsky's method for the postsynaptic AChE, apparently the majority of sprouting occurred at terminals (Fig. 1), although occasionally preterminal and nodal sprouting were also seen (results not shown). A sprout was more often elaborated at the distal end of a terminal branch than at the rest of the branch. The sprouts usually elongated and contacted the same muscle fiber, but sometimes they also extended to the neighboring fibers. Many sprouts lacked AChE reaction product along their entire length (Fig. 1, arrowhead) while others showed only a small ring of AChE staining (Fig. 1, upper arrow) at the end of the nerve process. The number of sprouts per junction varied from junction to junction. The length of each sprout ranged from a few microns to tens of microns (see Morphometry, below).

Changes of synaptic ECM in relation to the nerve terminal during NMJ growth and sprouting

To examine the remodeling of synaptic ECM in relation to the motor nerve terminals during axonal growth and sprouting, NMJs double labeled with 4-Di-2-Asp and TMR-PNA were viewed before and 2–3 months after nerve implantation. During the period between observations, elongation of existing branches and/or addition of new branches occurred at most of the NMJs. An example of the extensive change in both nerve terminal and synaptic ECM following nerve implantation is shown in Figure 2. Before nerve implantation, the nerve terminal staining (Fig. 2*a*) was accompanied by PNA staining (Fig. 2*b*). When the same junction was viewed the second time, 99 d after nerve implantation, two new terminal branches (20 μm and 55 μm, respectively) were added at the tip of a branch (arrowhead in Fig. 2*c*). PNA-stained ECM was also seen along these two new branches (arrowhead in Fig. 2*d*). The total length of this junction (sum of lengths of individual junctional branches) was increased by 36%. This example demonstrated the substantial growth and remodeling of the NMJ following nerve implantation, with the changes of synaptic ECM corresponding to that of nerve terminals.

Although correlation between the distribution of PNA staining and nerve terminal staining was commonly seen during junctional growth or sprouting, lack of correlation between these two synaptic labels was also observed. One example is shown in Figure 3. Initially, this junction had a compact configuration with synaptic ECM (Fig. 3*b*) accompanying the nerve terminal arbor (Fig. 3*a*) at each branch. The same junction viewed for the second time, 77 d after nerve implantation, revealed dramatic elongation of two nerve branches and the corresponding PNA-stained ECM (1, 2 in Fig. 3*c,d*). The growth of this junction was so dramatic that the total junctional length increased by 115%. One interesting feature of this junction is the elongation of PNA-stained ECM beyond the terminal by 50 μm at one branch (distance between arrow and arrowhead in Fig. 3*d*). However, the length of the nerve terminal at this branch remained unchanged over time (compare arrowheads in Fig. 3*a,c*), in contrast to the observations for branches 1 and 2.

PNA-stained ECM was not only seen extending beyond static nerve terminals but also seen ahead of nerve terminals that elongated during the interval between observations. One example is shown in Figure 4. The junction initially exhibited good alignment between nerve endings (Fig. 4*a*) and synaptic ECM (Fig. 4*b*). At the second observation, 67 d after nerve implantation, the same junction showed elongation of most of

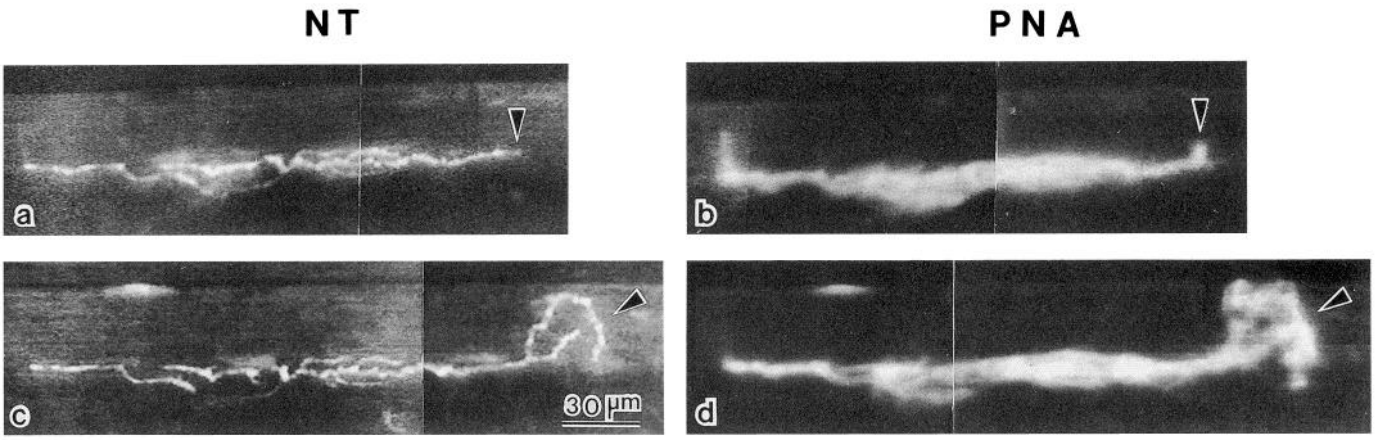

Figure 2. Formation of new nerve terminal branches and corresponding synaptic ECM after nerve implantation. *a* and *b*, Before nerve implantation, the NMJ was visualized with 4-Di-2-Asp (*a*) and TMR-PNA (*b*). *Arrowheads* indicate the regions that elongated later. *c* and *d*, The same junction was stained and visualized again, 99 d after nerve implantation. Two nerve terminal branches had emerged (*c, arrowhead*) and were apposed by the synaptic ECM labeled by PNA (*d, arrowhead*). In this and the following figures (Figs. 2–10), the *left panels* (*NT*) are images of nerve terminals from the initial and subsequent viewing(s) in order (*from top to bottom*), as revealed by 4-Di-2-Asp staining. The *right panels* (*PNA*) are images of synaptic ECM from the same fields of double-stained junctions in each viewing, as revealed by TMR-PNA. All images in the same figures have the same magnification unless otherwise indicated.

the terminal branches and even formation of a small nerve terminal branch (Fig. 4*c*, arrowhead). PNA-stained ECM also increased in length and correlated with the terminals, except at one branch where the synaptic ECM is about 40 μm longer than the nerve terminal (between arrow and arrowhead in Fig. 4*d*). In contrast to the junction shown in Figure 2, the above two junctions (Figs. 3, 4) exhibited noncorrelated changes between synaptic ECM and the nerve terminal during the induction of nerve sprouting. PNA-stained ECM often stretched tens of microns beyond the nerve terminal.

Elongation of the nerve sprouts along the extended synaptic ECM

The extended synaptic ECM shown above may provide a pathway for the growing nerve terminal to follow. If this is the case, one would expect to observe junctions with nerve terminals growing along the extended synaptic ECM. An example of this type of junctional dynamic is shown in Figure 5. Initially, PNA-stained ECM was aligned with the nerve terminal arbor, except at one branch where PNA staining (arrowhead in Fig. 5*b*) had

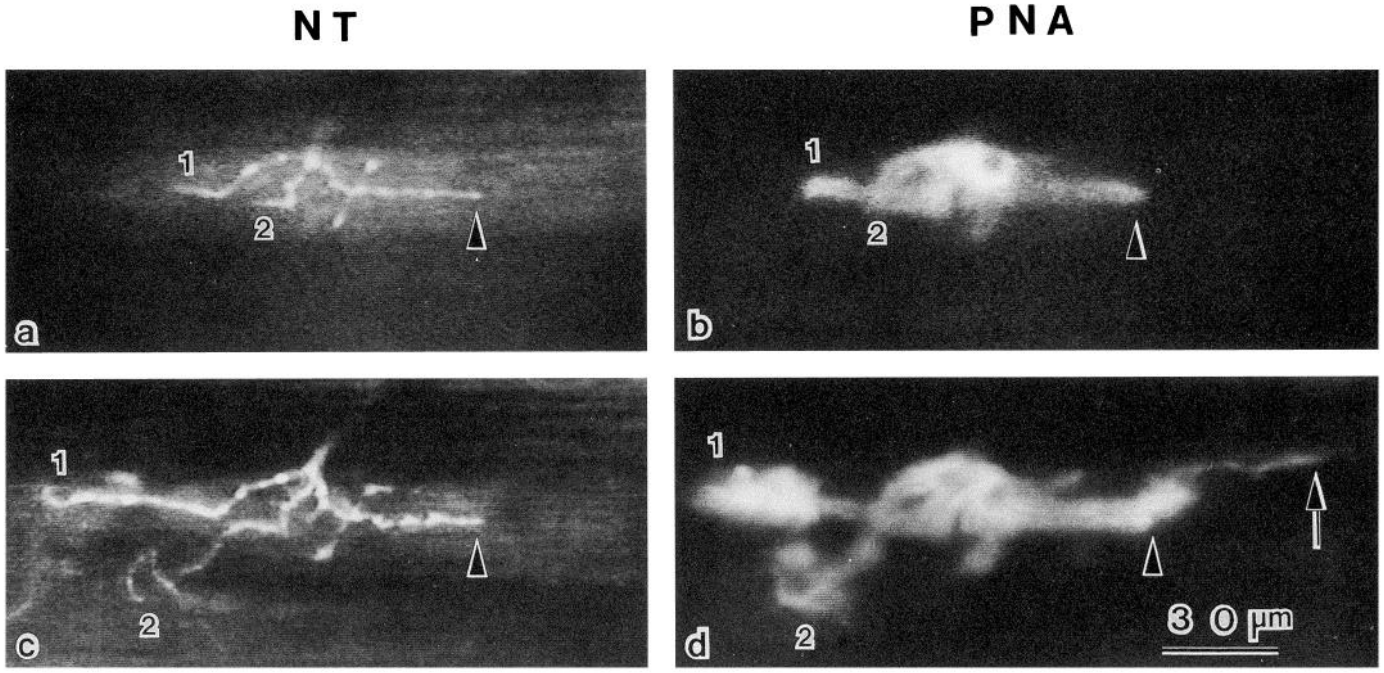

Figure 3. A lack of correlation between nerve terminal and synaptic ECM following nerve terminal sprouting. *a* and *b*, Views of the nerve terminal and corresponding synaptic ECM before nerve implantation. Markers (*1, 2*) indicate the branches that later changed. *c* and *d*, Views of the same junction, 77 d after nerve implantation. Branches *1* and *2* elongated dramatically with nerve terminals (*c*) corresponding to synaptic ECM (*d*). However, another branch (*arrowheads*) showed no changes in the nerve terminal length (compare *arrowheads* in *a* and *c*) but had an increase in the length of PNA-stained ECM (*arrow* in *d*).

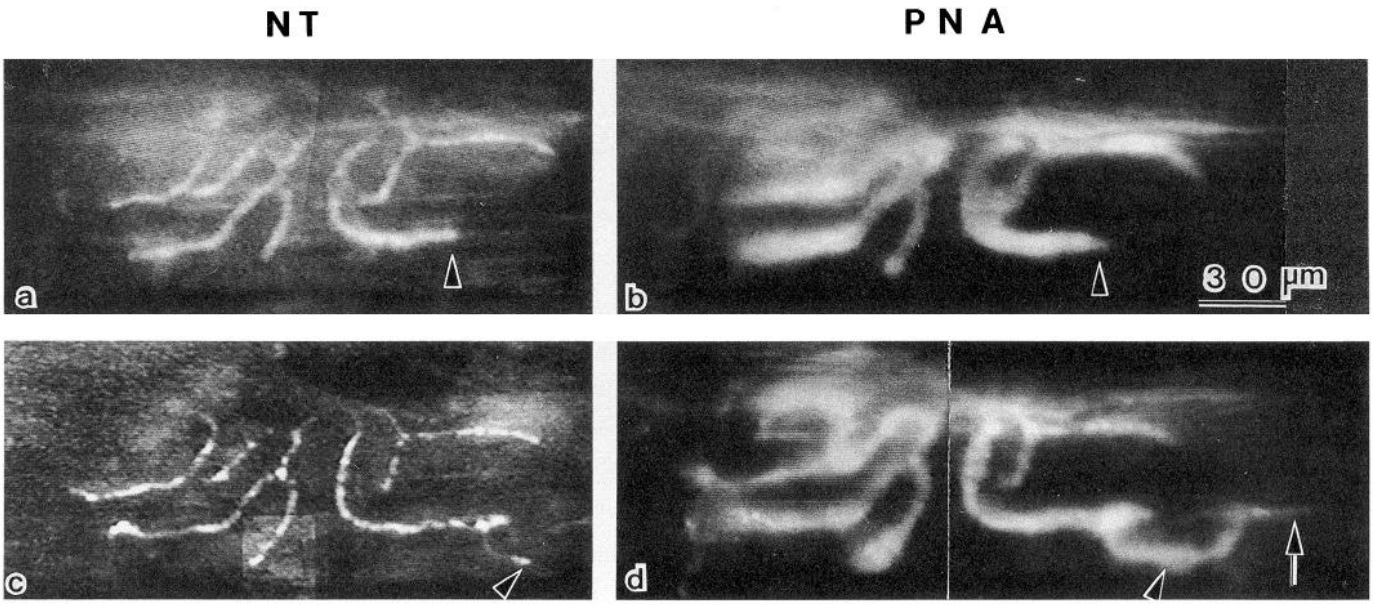

Figure 4. Extension of synaptic ECM beyond a newly formed nerve sprout. *a* and *b,* Initial view of the nerve terminal arborization and corresponding synaptic ECM. *Arrowheads* point to the tip of one branch from which a new nerve sprout later emerged. *c* and *d,* The second view, 67 d after nerve implantation. The formation of a small nerve branch (*c, arrowhead*) was evident but it was stained lightly by 4-Di-2-Asp. The region between *arrow* and *arrowhead* in *d* was devoid of nerve terminal.

already extended at least 20 μm beyond the terminal (arrowhead in Fig. 5*a*). At the second observation, 79 d after nerve implantation, the nerve terminal at the noncorrelated branch had grown into the extended ECM region (arrowhead in Fig. 5*c*). Along with the growth of the nerve terminal, PNA-stained ECM elongated even farther and bifurcated in front of the terminal ending (arrowheads in Fig. 5*d*). The elongated ECM was not caused by the experimental procedure since it was also observed at the beginning of the experiments (Fig. 5*b*). This result is similar to our previous finding on normal frog muscles that synaptic ECM longer than nerve terminals was seen in some NMJs without prior *in vivo* observations (Chen et al., 1991).

To examine further the dynamics of junctional growth, some junctions were viewed one more time after the second observation. As shown in Figure 6, before nerve implantation, the junction displayed nearly equal alignment between the nerve terminal (Fig. 6*a*) and synaptic ECM (Fig. 6*b*) at each branch. At the subsequent viewing, 64 d after induced sprouting, the PNA-stained ECM at one branch had elongated horizontally (arrowhead in Fig. 6*d* indicates the elongation point) and then bifurcated vertically. The nerve terminal branch did not show any changes (arrowhead in Fig. 6*c*). At the final viewing, 16 d later, the nerve terminal elongated horizontally by 10 μm (arrowhead in Fig. 6*e* indicates the elongation point). In addition,

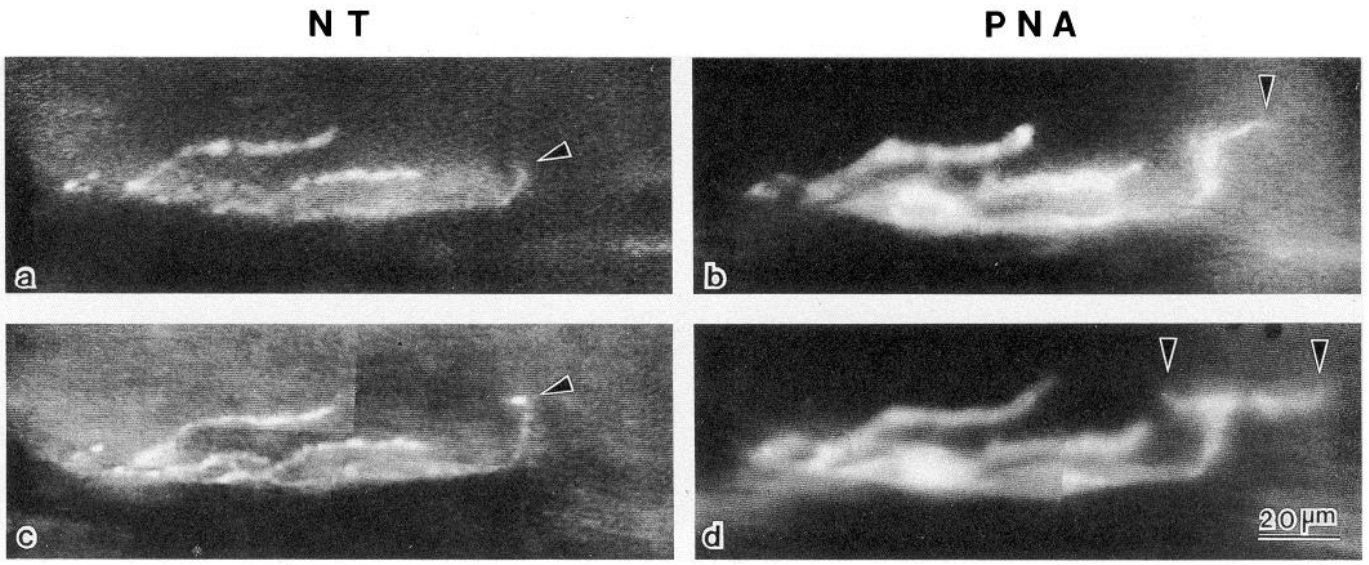

Figure 5. Nerve terminal growth along the extended synaptic ECM at an end plate viewed twice. *a* and *b,* The initial viewing of the nerve terminal and synaptic ECM, respectively. *Arrowheads* indicate PNA staining (*b*) longer than the terminal staining (*a*). *c* and *d,* The same junction at the second viewing, 79 d following nerve implantation. The nerve terminal elongated during this period of time (*c, arrowhead*). The synaptic ECM extended farther to new areas (*arrowheads*).

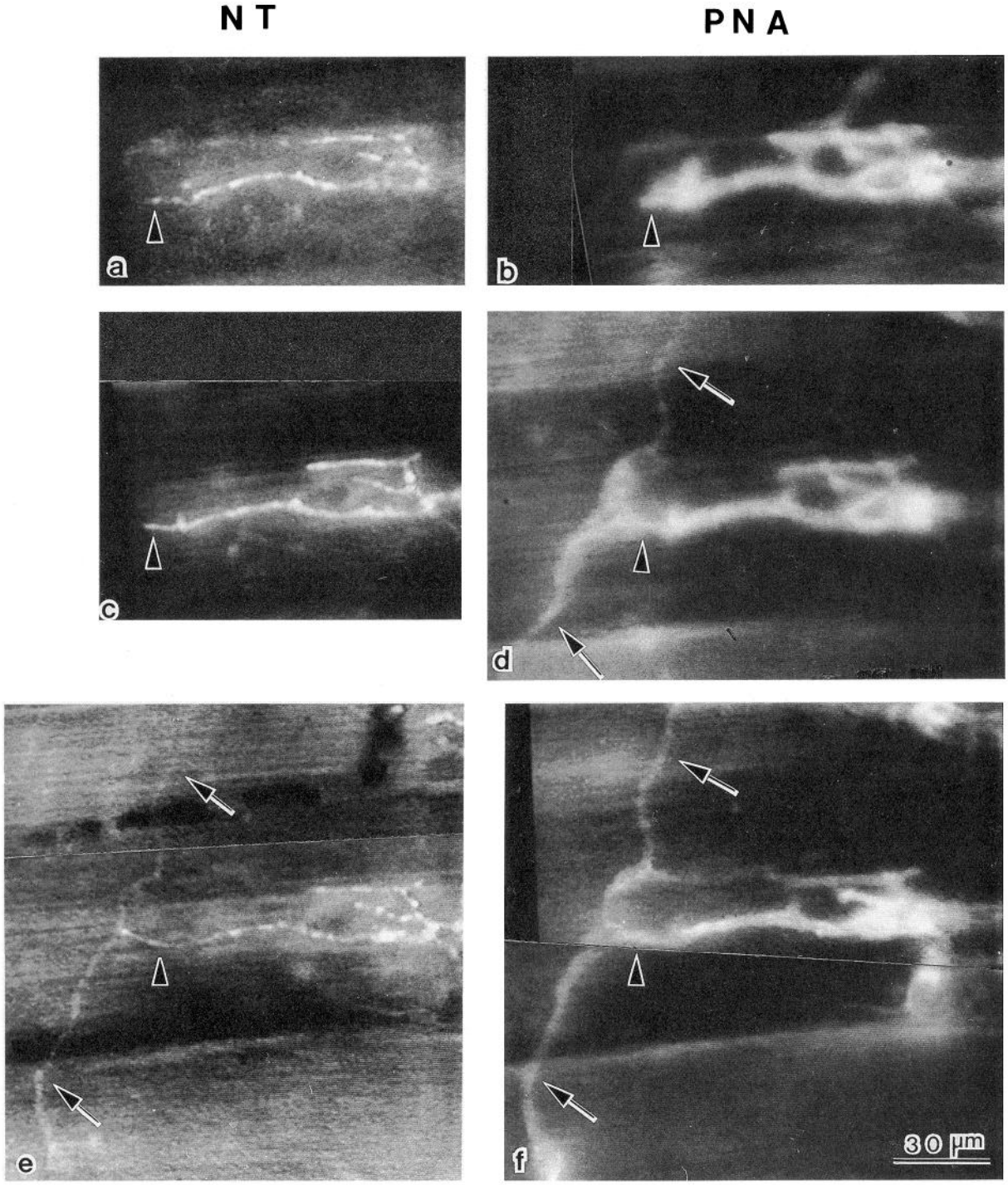

Figure 6. Nerve terminal growth along the extended synaptic ECM at an end plate viewed three times. *a* and *b,* The initial images of the nerve terminal and corresponding synaptic ECM. *Arrowheads* indicate the points from which the elongation of a branch later occurred. *c* and *d,* The second viewing, 64 d after nerve implantation. The nerve terminal remained unchanged (*arrowhead* in *c*) while synaptic ECM elongated dramatically (*arrows* in *d*). *e* and *f,* The final viewing, another 16 d later. The nerve terminal also elongated (*e, arrows*) to keep pace with synaptic ECM (*f, arrows*). The *arrowheads* in *c–f* indicate the same locations as those in *a* and *b.*

the bifurcating portion of PNA-stained region now also showed 4-Di-2-Asp staining (arrows in Fig. 6*e*). The crossing nerve fiber shown in this example could be a process from other types of neurons, such as autonomic or sensory neurons. If so, the above result would suggest that differentiation of PNA-stained ECM advances prior not only to motor nerve terminal but also to other neuronal processes. The above results also suggest that the lack of correlation between nerve terminal and synaptic ECM is a transient phenomenon. It appears likely that the nerve terminal would eventually grow into the region previously occupied only by the extended synaptic ECM.

Absence of postsynaptic AChE at the extended synaptic ECM region

As was noted in the previous study (Chen et al., 1991), the lack of correlation between PNA-stained ECM and the nerve ter-

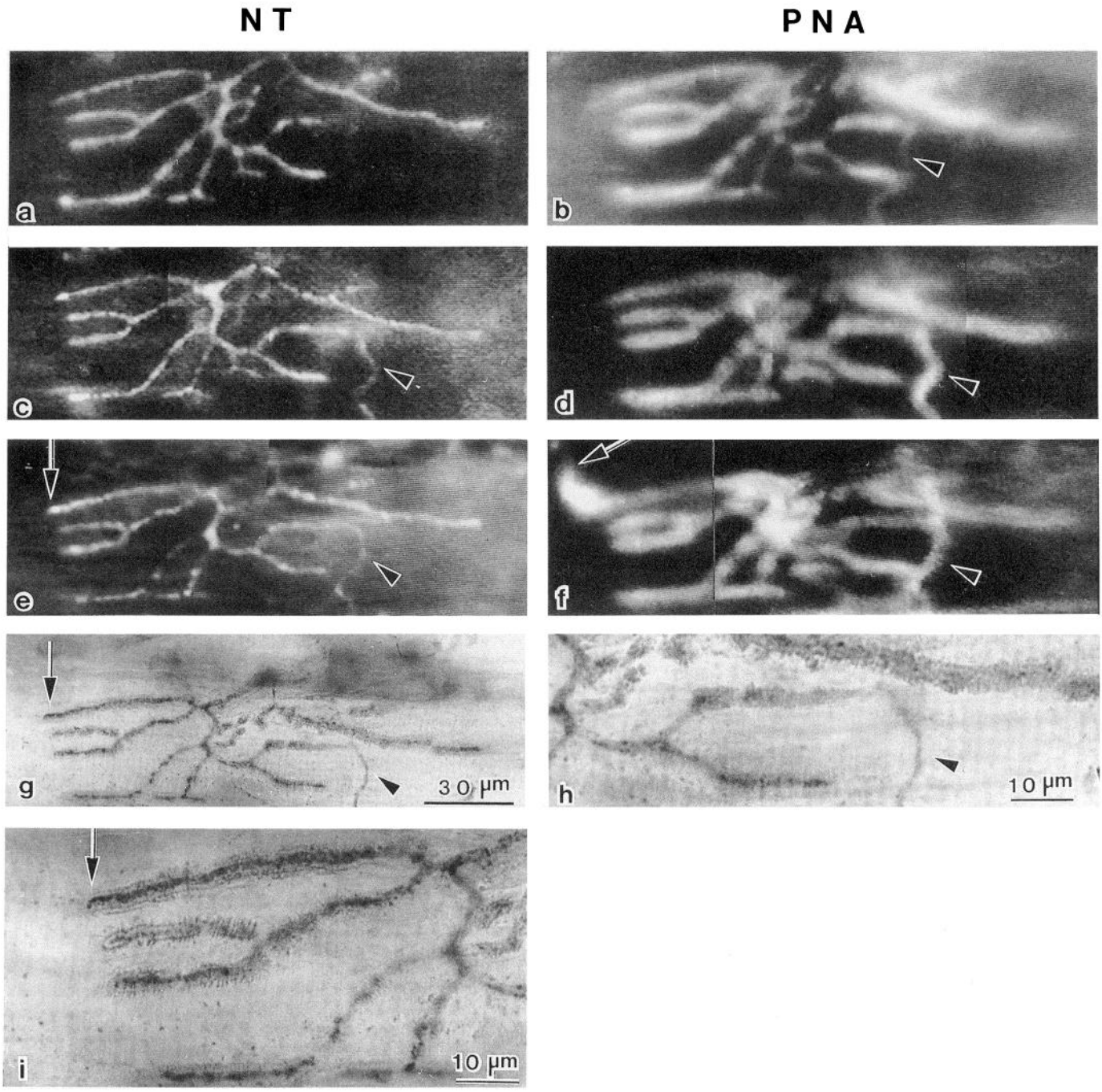

Figure 7. Absence of AChE at the extended synaptic ECM. *a* and *b*, The initial observation of a junction. The synaptic ECM was not overlain by nerve terminal at one region (*arrowhead* in *b*). *c* and *d*, The second viewing, 57 d after nerve implantation. A new nerve terminal branch (*arrowhead* in *c*) had grown into the previously existing ECM (*arrowhead* in *d*). *e* and *f*, The final viewing, 14 d after the second observation. Correlation between the nerve terminal and synaptic ECM was still maintained at this branch (*arrowheads*), while synaptic ECM was longer than the nerve terminal at the other branch (*arrows*). *g*, Histological staining delineated the nerve terminal and AChE. *h* and *i*, Higher magnification of two regions of *g*. The absence of AChE along the nerve process (*arrowheads* in *g*, *h*) indicates it is likely a newly formed sprout. AChE reaction product outlined the nerve terminal at the other branch (*arrows* in *g*, *i*), but no AChE was seen at the extended ECM region indicated by an *arrow* in *f*. Scale bar in *g* also applies to *a–f*.

minal seen above could be indicative of synaptic ECM preceding the outgrowth of the terminal, or alternatively due to the retraction of the nerve terminal leaving the synaptic ECM behind. To differentiate between these two possibilities, sartorius muscles were stained with NBT for nerve terminals and Karnovsky's method for postsynaptic AChE (see Materials and Methods) immediately after the final *in vivo* observations. As shown in Figure 7, the nerve terminal was initially correlated with the synaptic ECM at each individual branch except at one where the ECM was unopposed by the nerve terminal (arrowhead in Fig. 7*b* and corresponding region in Fig. 7*a*). The PNA staining at this branch was evident although it was less intense than at the other branches. Fifty-seven days after nerve implantation, a nerve terminal (arrowhead in Fig. 7*c*) occupied the extended

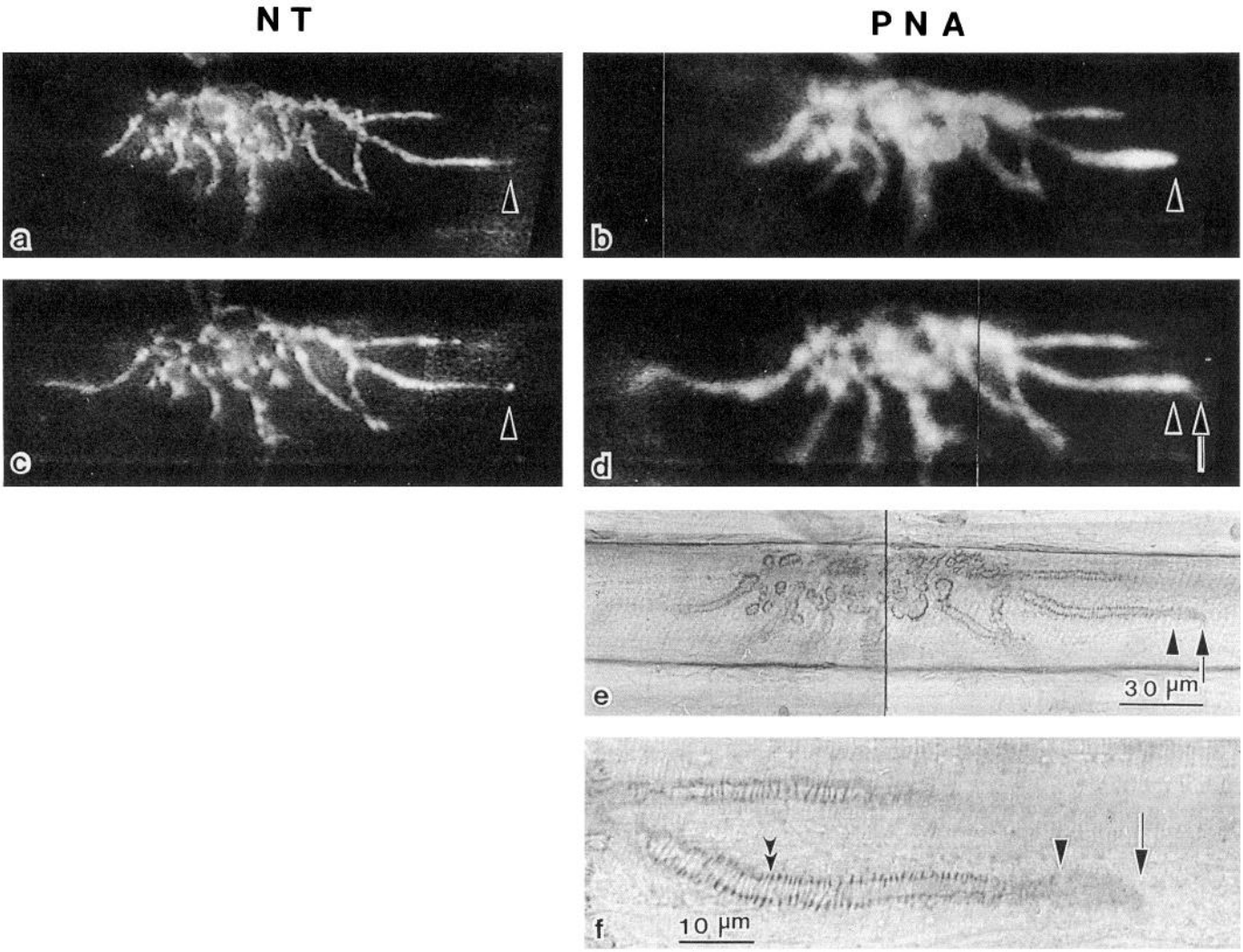

Figure 8. Absence of postsynaptic junctional folds at the region with extended synaptic ECM. *a* and *b,* Initial images of the nerve terminal and synaptic ECM. *c* and *d,* Images of the same junction, 68 d after nerve implantation. The junction elongated horizontally, but one nerve terminal branch remained unchanged (compare *arrowheads* in *a, c*). Note that the PNA staining was longer than the nerve terminal staining at this branch (distance between *arrowhead* and *arrow* in *d*). *e,* The same junction stained with HRP-PNA. *f,* Higher magnification of *e,* showing the right part of the junction. No distinctive junctional folds were seen at the region between *arrow* and *arrowhead,* which was unoccupied by the nerve terminal. The region innervated by the nerve terminal shows extensive junctional folds (*double arrowhead* in *f*). Scale bar in *e* also applies to *a–d.*

PNA-stained ECM region (arrowhead in Fig. 7*d*). This result, similar to Figure 6, also indicated that the lack of correlation between synaptic ECM and the nerve terminal was transient. At the final observation, 14 d later, the nerve terminal and synaptic ECM remained in good alignment at this branch (arrowheads in Fig. 7*e,f*). However, during this period, the ECM at another branch (arrow in Fig. 7*f*) elongated about 20 μm beyond the accompanying nerve terminal (arrow in Fig. 7*e*), which remained unchanged throughout the three observations.

Histological staining of this junction after the final *in vivo* observation revealed several interesting features. First, the shape of the nerve terminal, including the sprout, delineated by NBT staining was identical to that revealed by 4-Di-2-Asp, suggesting that the fluorescent nerve terminal dye labels all nerve terminal branches. Second, unlike the rest of the nerve terminal branches, the new nerve branch (arrowhead in Fig. 7*g,h*) lacked AChE staining. Such a "naked" terminal without accompanying AChE is thought to be a newly developed nerve sprout that has not yet induced formation of the postsynaptic AChE (Wernig et al., 1980). Finally, AChE was also missing from the region that contains only PNA-stained ECM without an overlying nerve terminal (arrow in Fig. 7*f,g*). A higher-magnification view of this branch (arrow in Fig. 7*i*) clearly showed nerve terminals outlined by AChE staining. However, at the extended, PNA-stained region (distal to the arrow in Fig. 7*i*), neither the nerve terminal nor AChE was seen. The lack of AChE implies that this extended ECM region was not previously occupied by a nerve that had later withdrawn. Otherwise, AChE remnants would be expected at the abandoned synaptic site (Wernig et al., 1980, 1981b). Therefore, the presence of the synaptic ECM beyond the nerve terminal is unlikely due to the retraction of the terminal. Instead, it may represent a growing junction with the differentiation of PNA-stained ECM occurring first.

Absence of junctional folds at the extended synaptic ECM region

In addition to the lack of AChE in the extended PNA-stained ECM regions, the regions are devoid of junctional folds, a mor-

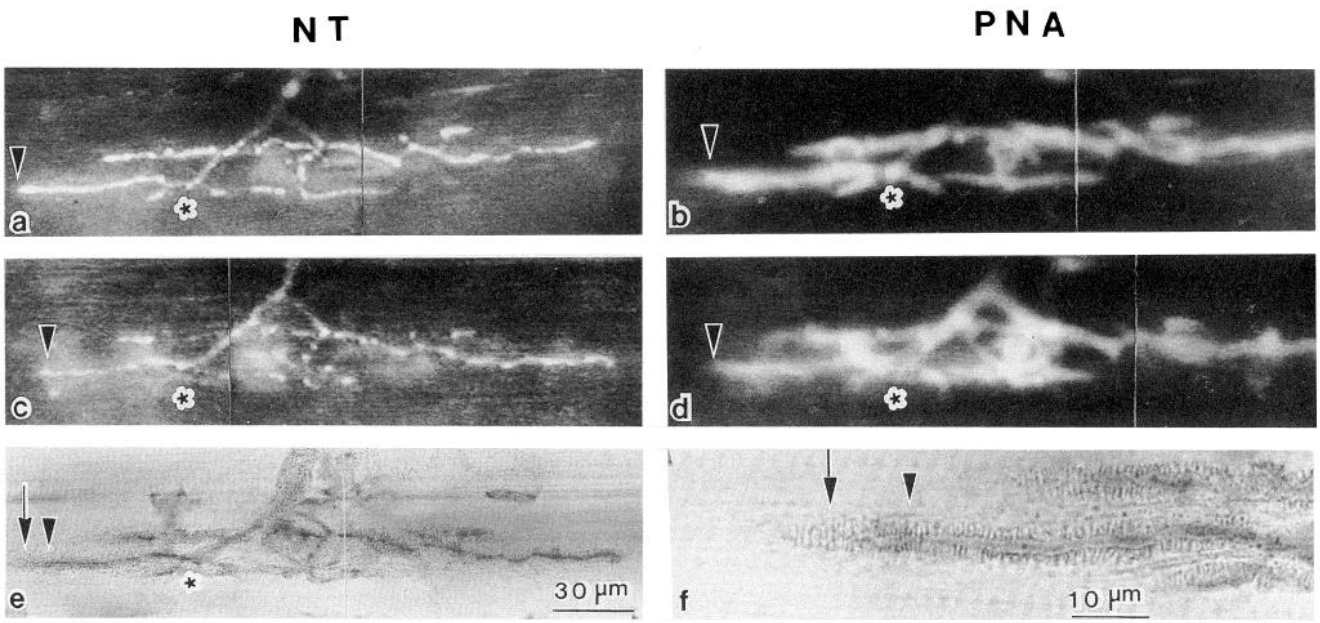

Figure 9. Remnants of AChE and junctional folds at the region with the retracting nerve terminal branch. *a* and *b*, The initial viewing of an end plate. Note the close correspondence between the nerve terminal and synaptic ECM (*arrowheads* in *a* and *b*). *c* and *d*, The second viewing, 55 d later. The nerve terminal underwent retraction and the *arrowheads* point to one shortened branch (compare *arrowheads* in *a, c*). However, PNA staining of the same branch was unchanged (compare *arrowheads* in *b, d*). *e* and *f*, The image of histological stains for the nerve terminal and AChE (*e*), also shown at higher magnification (*f*). *Arrowheads* point to the tip of the regressing nerve terminal. AChE reaction product and junctional folds were present at the abandoned gutter (*arrows*). Scale bar in *e* also applies to *a–d*.

phological marker for mature junctions. For example, a close correspondence of the nerve terminal staining with PNA staining was seen at the initial observation of the junction shown in Figure 8, *a* and *b*, although the terminal staining at one branch (arrowhead in Fig. 8*a*) was fainter near the tip than elsewhere. Sixty-eight days after nerve implantation, the nerve terminal at the same branch remained unchanged (arrowhead in Fig. 8*c*) while PNA-stained ECM increased in length, projecting 16 μm beyond the terminal (the distance between arrowhead and arrow in Fig. 8*d*). The same junction stained with HRP-PNA following the final observation is shown in Figure 8*e*. The extended ECM region displays a different staining pattern from the region that is occupied by the nerve terminal as depicted in the higher-magnification view (Fig. 8*f*). Specifically, the portion of the branch occupied by the nerve terminal has the appearance of parallel tracks crossed by small vertical bars. The vertical bars represent the junctional folds filled with HRP reaction product (double arrowhead in Fig. 8*f*). However, at the region containing the PNA-stained ECM without the overlying nerve terminal (region between arrow and arrowhead in Fig. 8*e,f*), no distinctive junctional folds as those seen in the innervated region were observed. It has been shown that junctional folds persist long after the retraction of the nerve terminal (Wernig et al., 1980). In contrast, junctional folds are missing or less developed at the newly formed sprout region (Wernig et al., 1980, 1981a; Anzil et al., 1984). The absence of distinctive junctional folds at the extended ECM region further suggests that this junction is most likely undergoing growth with PNA-stained ECM extending first.

In comparison with the junction shown above, a few NMJs that had undergone nerve retraction while between observations showed extensive junctional folds as well as AChE at the abandoned sites. An example is illustrated in Figure 9. The junction initially showed a good correlation between the nerve terminal (Fig. 9*a*) and the synaptic ECM (Fig. 9*b*). Over a period of 55 d, the nerve terminals withdrew from some regions (arrowhead in Fig. 9*c*). However, the synaptic ECM showed little change in length (arrowhead in Fig. 9*d*). As a result of nerve retraction, the PNA-stained ECM was about 10 μm longer than the terminal (compare the distance between arrowhead and asterisk in Fig. 9*c,d*). Histological examination of this region (between arrow and arrowhead in Fig. 9*e*) confirmed the absence of the nerve terminal. In addition, as shown in the higher-magnification view of this region, the "empty" gutter contained junctional folds and AChE reaction products (arrow in Fig. 9*f*). In contrast to the junction shown in Figure 8, the presence of AChE and the junctional folds suggests that this "empty" synaptic ECM region is probably the result of nerve terminal retraction rather than synaptic ECM leading nerve terminal growth (see Discussion).

Continual elongation of synaptic ECM over time

Additional evidence supporting the hypothesis that extension of synaptic ECM precedes neurite outgrowth during remodeling was obtained by the observations that dramatic changes in the synaptic ECM but not in nerve terminals occur following the nerve implantation. For example, a triple observation of an NMJ during a total of 77 d of nerve implantation revealed only slight elongation at one nerve terminal branch (Fig. 10*a,c,e*). PNA-stained ECM at the same branch began to elongate (although slightly) by the time of the second observation (arrowhead in Fig. 10*d*) and continued to grow. Within the next 10 d, the PNA-stained region extended more than 60 μm beyond the nerve terminal (compare the arrowheads in Fig. 10*e,f*). This example demonstrated the dramatic elongation of PNA-stained ECM ahead of the nerve terminal even in a relatively short period of time.

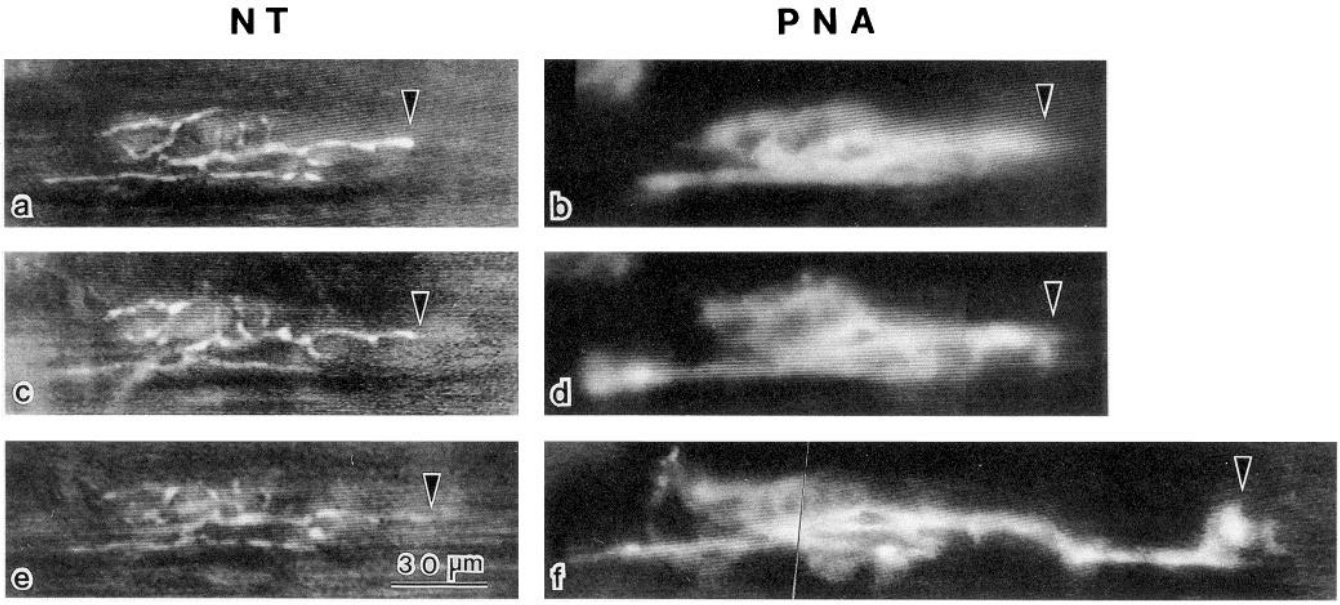

Figure 10. A triple observation of an end plate showing a drastic growth of synaptic ECM but only a slight change in the nerve terminal. *a* and *b*, The initial images. *c* and *d*, The subsequent images of 67 d later. *e* and *f*, The final images, another 10 d later. *Arrowheads* in *a*, *c*, and *e* indicate the end of a nerve terminal branch, which slightly increased in length over time. *Arrowheads* in *b*, *d*, and *f* indicate the changes of synaptic ECM at that branch. The change is especially significant after the second observation.

Synaptic ECM longer than the nerve terminal visualized by TTC

Fine nerve processes, such as lamellipodia and filopodia, can be visualized by fluorescent-labeled TTC (Robbins and Polak, 1988). This dye stains the nerve terminal membrane and is nontoxic when used under low intensity of illumination and short light exposure time (Hill and Robbins, 1991). Therefore, FITC-conjugated TTC was used along with TMR-PNA to exclude the possibility that the lack of correlation between the nerve terminal and synaptic ECM was an artifact produced by the inability of 4-Di-2-Asp to stain fine nerve processes. As shown in Figure 11, the noncorrespondence between FITC-TTC and TMR-PNA was also apparent (compare arrowheads in Fig. 11*a* with arrows in *b*). PNA-stained ECM is about 14 μm (distance between arrows and arrowheads in Fig. 11*b*) longer than the corresponding terminals. Using FITC-TTC, we have examined more than 100 NMJs in five normal sartorius muscles and found 18 of them exhibiting PNA-stained ECM longer than nerve terminals. Thus, the noncorrelation between the synaptic ECM and nerve terminals is not unique to 4-Di-2-Asp staining.

Morphometry

To determine quantitatively the efficiency of the nerve implantation in inducing nerve sprouting, we examined the frequency and extent of nerve sprouting in frog NMJs after nerve implantation. For a total of 167 junctions (in 10 frogs) that were stained with the histological methods after the repeated *in vivo* observations, signs of sprouting (see Material and Methods for definition) were found in 46% of NMJs (77 of 167). The number of sprouts varied from 0 to 10 sprouts at each NMJ with an average of 1.06 sprouts per junction. Some of the junctions showed dramatic growth and sprouting. The length of sprouts ranged from 3 μm to 97 μm, with the mean value of 17 μm. These results indicate that nerve implantation was very effective in inducing axonal sprouting in frog muscles as shown previously (Diaz and Pecot-Dechavassine, 1990).

The distribution of synaptic ECM in relation to the nerve terminal was examined in 167 NMJs. Of these junctions, 65% (108 of 167) showed at least one junctional branch extending with PNA-stained ECM longer than the nerve terminal. All

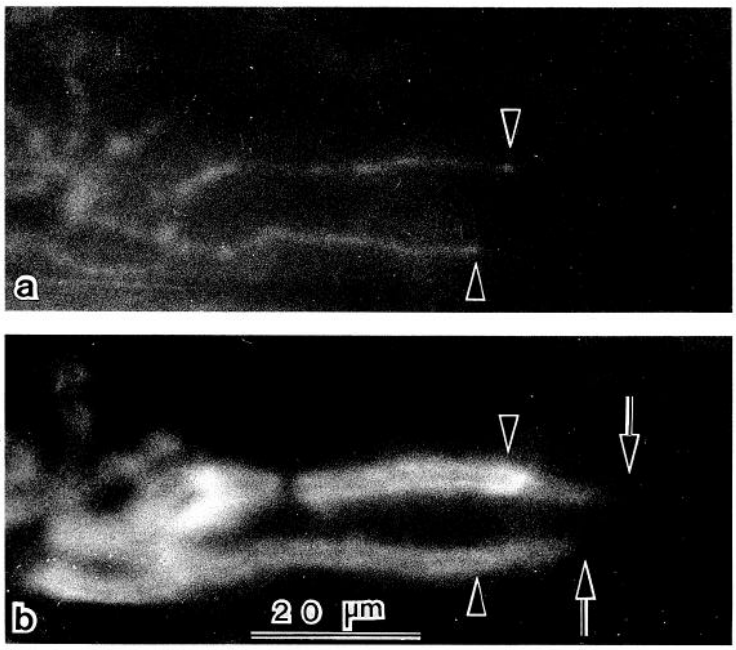

Figure 11. Noncorrespondence between the nerve terminal and synaptic ECM at a normal frog NMJ revealed by double staining with FITC-TTC and TMR-PNA. *a*, The nerve terminal visualized by FITC-TTC. *b*, The synaptic ECM visualized by TMR-PNA. The lack of correlation between these two synaptic elements is apparent at the regions indicated between *arrowheads* and *arrows*.

these elongated regions were lacking postsynaptic AChE and junctional folds. The frequency of the noncorrespondence between nerve terminals and PNA-stained ECM following nerve implantation is much higher than that in normal frog NMJs (9.5% of normal junctions show mismatch) (Chen et al., 1991).

We have also examined the distribution of synaptic ECM in relation to the nerve terminal at individual junctional branches that showed nerve terminal sprouting. For a total of 187 newly formed sprouting branches at 167 junctions, 71% of sprouts (132 of 187) are correlated with the PNA-stained ECM. Twenty-nine percent of sprouts (54 of 187) had PNA-stained ECM extending beyond the end of the nerve terminal by at least 5 μm. Postsynaptic AChE and junctional folds were missing at the extended ECM regions of all synaptic regions examined. Out of 187 sprouts, only one sprout (0.5%) extended 5 μm past the confines of the corresponding ECM.

Discussion

The present study has demonstrated the remodeling of synaptic ECM in relation to nerve terminal sprouts in adult living NMJs with repeated *in vivo* observations. This work has provided new findings consistent with our previous hypothesis that extension of synaptic ECM precedes nerve terminal growth during synaptic remodeling. In the previous study, we found synaptic ECM longer than nerve terminals in approximately 10% of normal adult NMJs (Chen et al., 1991). In contrast, 65% of NMJs in the present study had at least one branch with synaptic ECM longer than the nerve terminal following the induced sprouting. At the extended synaptic ECM region, the absence of nerve terminals was confirmed by NBT histological staining and TTC fluorescent staining. In addition, the postsynaptic specializations such as AChE staining and junctional folds were not detected with light microscopy at the extended synaptic ECM region. Thus, this region is not likely a junctional remnant resulting from nerve terminal retraction. Instead, it is more likely a region with synaptic ECM leading the nerve terminal. This is further supported by the finding of continual extension of synaptic ECM with little change in the nerve terminal length in some junctions. In addition, we have seen nerve terminals that eventually colocalized with previously extended synaptic ECM. These results suggest that the synaptic ECM molecules recognized by PNA are expressed before, and may play a role in, the extension of nerve terminals during synaptic remodeling.

Induction of axonal sprouting in frog sartorius muscle

In addition to the demonstration of synaptic remodeling in living NMJs, the present study has further confirmed that nerve implantation is an effective method to induce nerve terminal sprouting in the frog NMJ. Motor nerve terminal sprouting occurs in mammalian and frog skeletal muscles following partial denervation or exposure to neurotoxins like TTX, botulinum toxin, α-bungarotoxin, formamide, or curare (Wernig et al., 1980; Brown et al., 1981; Wines and Letinsky, 1988; Diaz and Pecot-Dechavassine, 1989; Diaz et al., 1989). Sprouting of the nerve terminal can also be induced simply by placing a segment of the sciatic nerve on the surface of frog cutaneous pectoris muscle (Diaz and Pecot-Dechavassine, 1990). We used the same method and also found extensive nerve sprouting in frog sartorius muscles within 2–3 months of implantation of nerve segments. Signs of sprouting were found in 46% of NMJs examined. The occurrence of sprouting after nerve implantation is higher than in normal unoperated frog muscles (20–28%; see Herrera and Scott, 1985). The results indicate that nerve implantation is a simple and yet powerful method to induce nerve terminal sprouting in frog skeletal muscles without the use of toxins. This approach allowed us to examine the dynamic changes of synaptic ECM recognized by PNA during the active growth of the nerve terminal.

The dynamic relationship between synaptic ECM and the nerve terminal outgrowth

In our previous study on remodeling of synaptic ECM in normal frog NMJs, synaptic ECM longer than nerve terminals was seen in junctional branches that elongated as well as in those that retracted during the observation intervals (Chen et al., 1991; Ko, 1991). Thus, questions regarding the origin of the elongated synaptic ECM were raised. Was this region of synaptic ECM once occupied by a nerve terminal that had retracted, or did it represent a newly differentiated region that would be followed by nerve terminal outgrowth? To distinguish between these two alternatives, fluorescent staining was combined with NBT/AChE histological staining. In the previous study, we saw two different types of extended, PNA-stained regions in normal NMJs: one showed AChE remnants, likely indicating abandoned synaptic sites, whereas the other type was devoid of AChE deposits, probably representing newly developed regions prior to nerve outgrowth. However, these NMJs were not observed repeatedly using the *in vivo* imaging method prior to NBT/AChE staining; therefore, their histories of dynamic changes were not clear and the results could not distinguish the association of extended synaptic ECM with growing nerve terminals versus regressing ones.

To address the above concern, we have combined repeated *in vivo* observations with histological staining in the present study. AChE and junctional folds revealed by histological staining have long been used as markers for mature NMJs. These postsynaptic specializations can persist for a long time (even years in frog muscle) at denervated synaptic sites (Krause and Wernig, 1985; Anzil and Wernig, 1989). Thus, "empty" synaptic gutters with the presence of AChE remnants and junctional folds seen in some frog NMJs are thought to be due to nerve retraction (Wernig et al., 1980, 1981b; Anzil et al., 1984). In contrast, nerve terminal branches without accompanying AChE staining or with only a few small ring-like arrangements of AChE staining found in some NMJs are interpreted as sprouts (Wernig et al., 1980, 1981a; Anzil et al., 1984). In concert with these interpretations of static images shown by histological staining, the present study has provided dynamic images of junctional plasticity in living NMJs. We found junctional folds revealed by AChE staining (Fig. 9*e,f*) in the region of the branch that showed retraction, but neither AChE nor distinctive junctional folds were seen in the region of the branch that displayed extension with synaptic ECM longer than the growing nerve terminal (Figs. 7, 8). Although we cannot exclude the possibility of less developed junctional folds at the light microscopic level, no distinctive junctional folds like those found in the innervated regions or retracted regions were seen in the elongated PNA-stained region. Thus, the absence of AChE and distinctive junctional folds from the extended synaptic ECM regions makes it unlikely that these regions were occupied previously by a nerve terminal that had retracted. Otherwise, one should observe AChE remnant and junctional folds at these regions. However, one could argue that, during the interval of observations, nerve terminals may have extended and rapidly induced the expression of PNA-

binding molecules, but retracted before AChE and junctional folds were formed. If this were the case, it would be difficult to explain the findings of multiple examples showing extension of synaptic ECM with little change in the nerve terminal length in successive observations (e.g., Figs. 3*a,c*; 6*a,c*; 7*a,c,e,g*; 8*a,c*; 10*a,c,e*). It seems highly unlikely that nerve terminals would extend tens or even hundreds of microns and induce only PNA-stained ECM, then retract to exactly the same points at various times of observation, as seen in so many examples (also see Figs. 6*c,e*; 7*a,c* in Chen et al., 1991; Fig. 5*a,c* in Ko, 1991). Instead, it is more likely that the PNA-stained ECM differentiates before the nerve terminal outgrowth, as proposed previously. This is further supported by the present results showing elongation of nerve terminals along the preceding synaptic ECM (Figs. 5, 6, 7; see also Fig. 7 in Chen et al., 1991).

Our results also showed that 65% of NMJs had at least one branch with synaptic ECM longer than the nerve terminal, in contrast to 9.5% of NMJs in normal muscles (Chen et al., 1991). Thus, nerve implantation has not only induced nerve terminal sprouting but also increased the chance of finding mismatch during the active nerve terminal extension, as predicted from our hypothesis. Among all newly formed junctional branches, 29% of them exhibited elongated synaptic ECM. The rest of the branches showed correlated changes between nerve terminals and PNA-stained ECM. These results imply that the lack of correlation between these two synaptic components may be a transient event. As predicted, the nerve terminal would later follow the pathways of PNA-stained ECM to match the change of synaptic ECM (Figs. 6, 7). Thus, depending on the timing of observation, match of both nerve terminal and synaptic ECM is anticipated in many of the NMJs that have undergone extension. The results are not contradictory to our hypothesis.

Finally, our results indicated that the extension of nerve terminal followed by synaptic ECM seems unlikely, even during active nerve growth (e.g., sprouting). If this were the case, we would have observed more cases showing nerve terminal staining longer than the synaptic ECM. However, nerve terminal extending beyond the confines of synaptic ECM was seen in only 1 of 187 sprouts examined (0.5%). Even in this case, the nerve terminal was only 5 μm longer than the PNA staining. This minor difference can probably be explained by the more diffuse distribution of synaptic ECM sometimes seen at the tip of a growing junctional branch (e.g., Fig. 4*d* in Chen et al., 1991). It is possible that, in this junction, synaptic ECM was present but was distributed too diffusely to be seen with PNA staining. Regardless of what the explanation may be for this one junction, the rest of the NMJs examined did not show nerve terminal longer than synaptic ECM, a result similar to our previous finding in normal frog NMJs (Chen et al., 1991). These results are consistent with the suggestion that the extension of synaptic ECM precedes nerve terminal outgrowth during synapse remodeling.

The reliability of 4-Di-2-Asp staining.

In both our previous and present studies, 4-Di-2-Asp was used in combination with fluorescent PNA to reveal, respectively, the presynaptic nerve terminal and synaptic ECM components at frog NMJs. Since 4-Di-2-Asp stains intracellular mitochondria (Magrassi et al., 1987), a concern is that 4-Di-2-Asp may not label very fine nerve processes because there may be few or no mitochondria. On the other hand, some studies have demonstrated the general reliability of this mitochondrial dye for the normal nerve terminal as well as for the branches that are undergoing growth and sprouting (Lichtman et al., 1987; Herrera and Banner, 1990). In order to ensure that noncorrespondence between the nerve terminal and synaptic ECM seen in our experiments was not due to the inability of 4-Di-2-Asp to stain thin nerve processes, NBT staining was performed following the final *in vivo* observation to confirm the 4-Di-2-Asp staining. In comparison with fluorescent dyes, NBT staining is believed to stain the entire length of the nerve terminal processes, including the filopodia of growing terminals as well as nerve terminals at the early stage of regeneration (Letinsky and DeCino, 1980; DeCino, 1981; Herrera et al., 1985; Herrera and Banner, 1990). We observed a close correspondence between these two types of nerve terminal stains in *all* of the junctions examined, including those undergoing sprouting (Fig. 7). The results, therefore, suggest that the extension of the synaptic ECM beyond the nerve terminal seen *in vivo* is unlikely due to the inability of 4-Di-2-Asp to stain thin nerve processes. This notion is further strengthened by a study using electron microscopy that showed the absence of nerve terminals at the extended PNA-stained region (Ko et al., 1992). Additional evidence showing noncorrespondence between nerve terminals and synaptic ECM is derived from combined application of fluorescent TTC and PNA. Fluorescent TTC, a probe that labels nerve terminal membranes, has been shown to stain very fine nerve processes such as filopodia and lamellipodia (Robbins and Polak, 1988). Extended PNA-stained regions without nerve terminals were also apparent when end plates were stained with fluorescently labeled TTC and PNA (Fig. 11). Thus, the lack of correlation between synaptic ECM and nerve terminals in this region is not due simply to an inability of 4-Di-2-Asp to stain fine nerve processes.

Possible mechanisms of synaptic remodeling

The concept that extension of synaptic ECM precedes the nerve terminal growth during synaptic remodeling suggests that the ECM molecules recognized by PNA may play a role in the extension of nerve terminals. This suggestion is compatible with studies of the roles of the other ECM molecules in axonal outgrowth (Sanes, 1989). However, how synaptic ECM extends ahead of the nerve terminal growth is unknown. In our previous study, the possibility of the involvement of Schwann cells in this process was raised (Chen et al., 1991). Such a speculation was based mainly on the fact that PNA staining was distributed primarily around Schwann cells at frog NMJs (Ko, 1987). One idea was that the extended PNA-stained region may be indicative of Schwann cell processes projecting out beyond the nerve terminal. This idea is supported by a previous study using electron microscopy. Anzil et al. (1984) showed that Schwann cell processes extended several microns ahead of the nerve terminals thought to be undergoing growth based on the histology of *fixed* muscle. Using repeated *in vivo* observations combined with electron microscopy, we have also shown recently that Schwann cell processes are longer than the nerve terminal at the extended, PNA-stained region (Ko et al., 1992). The idea that Schwann cells lead the nerve outgrowth is also agreeable to the finding that glial cells appear before the first nerve growth cones and may provide guidance cues during embryonic development in *Drosophila* (Jacobs and Goodman, 1989). Schwann cells have been shown to synthesize and secrete ECM molecules (Bunge et al., 1986; Chiu et al., 1991). Thus, it is possible that during the growth or sprouting of terminal branches, a Schwann cell

sends out its processes and releases PNA-binding molecules (PNA-BMs), which may subsequently influence neurite outgrowth. We have recently identified a 30 kDa PNA-BM from synapse-rich electric organs of *Torpedo* (Xiao et al., 1993). Antibodies against this PNA-BM also recognize the synaptic ECM in the frog NMJ. However, the function of this PNA-BM in synaptic formation and remodeling, and whether PNA-BMs are indeed released by Schwann cells remain to be examined.

In conclusion, the present work has provided direct evidence of the remodeling of synaptic ECM and its dynamic relationship with sprouting nerve terminals *in vivo*. The results are consistent with the concept that synaptic ECM precedes nerve terminal outgrowth and may play a role in nerve terminal plasticity. This new concept may lead to further insights into the mechanisms of synaptic remodeling.

References

Anzil AP, Wernig A (1989) Muscle fibre loss and reinnervation after long-term denervation. J Neurocytol 18:833–845.

Anzil AP, Bieser A, Wernig A (1984) Light and electron microscopic identification of nerve terminal sprouting and retraction in normal adult frog muscle. J Physiol (Lond) 350:393–399.

Balice-Gordon RJ, Lichtman JW (1990) *In vivo* visualization of the growth of pre- and postsynaptic elements of neuromuscular junctions in the mouse. J Neurosci 10:894–908.

Brown M, Holland RL, Hopkins WG (1981) Motor nerve sprouting. Annu Rev Neurosci 4:17–42.

Bunge RP, Bunge MB, Eldridge CF (1986) Linkage between axonal ensheathment and basal lamina production by Schwann cells. Annu Rev Neurosci 9:305–328.

Chen L, Ko CP (1991) Remodeling of synaptic extracellular matrix during nerve terminal sprouting in living frog neuromuscular junctions. Soc Neurosci Abstr 17:735.

Chen L, Folsom DB, Ko CP (1991) The remodeling of synaptic extracellular matrix and its dynamic relationship with nerve terminals at living frog neuromuscular junctions. J Neurosci 11:2920–2930.

Chiu AY, Espinosadelos-Monteros A, Cole RA, Loera S, deVellis J (1991) Laminin and s-laminin are produced and released by astrocytes, Schwann cells and Schwannomas in culture. Glia 4:11–24.

DeCino P (1981) Transmitter release properties along regenerated nerve processes at the frog neuromuscular junction. J Neurosci 1:308–317.

Diaz J, Pecot-Dechavassine M (1989) Terminal nerve sprouting at the frog neuromuscular junction induced by prolonged tetrotoxin blockade of nerve conduction. J Neurocytol 18:39–46.

Diaz J, Pecot-Dechavassine M (1990) Nerve sprouting induced by a piece of peripheral nerve placed over a normally innervated frog muscle. J Physiol (Lond) 421:123–133.

Diaz J, Molgo J, Pecot-Dechavassine M (1989) Sprouting of frog motor nerve terminals after long-term paralysis by botulinum type A toxin. Neurosci Lett 96:127–132.

Herrera AA, Banner LR (1990) The use and effects of vital fluorescent dyes: observation of motor nerve terminals and satellite cells in living frog muscles. J Neurocytol 19:67–83.

Herrera AA, Scott DR (1985) Motor axon sprouting in frog sartorius muscles is not altered by contralateral axotomy. J Neurocytol 14:145–156.

Herrera AA, Werle MJ (1990) Mechanisms of elimination, remodeling, and competition at frog neuromuscular junctions. J Neurobiol 21:73–98.

Herrera AA, Grinnell AD, Wolowske B (1985) Ultrastructural correlates of experimentally altered transmitter release efficacy in frog motor nerve terminals. Neuroscience 16:491–500.

Herrera AA, Banner LR, Nagaya N (1990) Repeated, *in vivo* observation of frog neuromuscular junctions: remodeling involves concurrent growth and retraction. J Neurocytol 9:85–99.

Hill RR, Robbins N (1991) Mode of enlargement of young mouse neuromuscular junctions observed repeatedly *in vivo* with visualization of pre- and postsynaptic borders. J Neurocytol 20:183–194.

Jacobs JR, Goodman CS (1989) Embryonic development of axon pathways in the *Drosophila* CNS. I. A glial scaffold appears before the first growth cones. J Neurosci 9:2402–2411.

Karnovsky MJ (1964) The localization of cholinesterase activity in rat cardiac muscle by electron microscopy. J Cell Biol 23:217–232.

Ko CP (1987) A lectin, peanut agglutinin, as a probe for the extracellular matrix in living neuromuscular junctions. J Neurocytol 16: 567–576.

Ko CP (1991) Peanut agglutinin as a probe for studying remodeling and differentiation of synaptic extracellular matrix at the frog neuromuscular junctions. In: Plasticity of motorneuronal connections (Wernig A, ed), pp 51–62. Amsterdam: Elsevier.

Ko CP, Chen L, Thompson A (1992) Synaptic remodeling revealed by combined video-enhanced fluorescent microscopy and electron microscopy of identified frog neuromuscular junctions. Soc Neurosci Abstr 18:218.

Krause M, Wernig A (1985) The distribution of acetylcholine receptors in the normal and denervated neuromuscular junction of the frog. J Neurocytol 13:765–780.

Letinsky MS, DeCino P (1980) Histological staining of pre- and postsynaptic components of amphibian neuromuscular junctions. J Neurocytol 9:305–320.

Lichtman JW, Magrassi L, Purves D (1987) Visualization of neuromuscular junction over periods of several months in living mice. J Neurosci 7:1215–1222.

Magrassi L, Purves D, Lichtman JW (1987) Fluorescent probes that stain living nerve terminals. J Neurosci 7:1207–1214.

Pecot-Dechavassine M, Diaz J (1991) Peripheral nerve segments induce sprouting in normally innervated frog muscle. In: Plasticity of motorneuronal connections (Wernig A, ed), pp 291–298. Amsterdam: Elsevier.

Purves D (1989) Assessing some dynamic properties of the living nervous system. Q J Exp Physiol 74:1089–1105.

Reichardt LF, Tomaselli KJ (1991) Extracellular matrix molecules and their receptors: functions in neural development. Annu Rev Neurosci 14:531–570.

Robbins N, Polak J (1988) Filopodia, lamellipodia, and retractions at mouse neuromuscular junctions. J Neurocytol 17:545–561.

Sanes JR (1983) Roles of extracellular matrix in neural development. Annu Rev Physiol 45:581–600.

Sanes JR (1989) Extracellular matrix molecules that influence neural development. Annu Rev Neurosci 12:491–516.

Wernig A, Herrera AA (1986) Sprouting and remodeling at the nerve–muscle junction. Prog Neurobiol 27:251–291.

Wernig A, Pecot-Dechavassine M, Stover H (1980) Sprouting and regression of the nerve at the frog neuromuscular junction in normal conditions and after prolonged paralysis with curare. J Neurocytol 9:277–303.

Wernig A, Anzil AP, Bieser A (1981a) Light and electron microscopic identification of a nerve sprout in muscle of normal adult frog. Neurosci Lett 21:261–266.

Wernig A, Anzil AP, Schwarz U (1981b) Abandoned synaptic sites in muscles of normal adult frog. Neurosci Lett 23:105–110.

Wigston DJ (1989) Remodeling of neuromuscular junction in adult mouse soles. J Neurosci 9:639–647.

Wigston DJ (1990) Repeated *in vivo* visualization of neuromuscular junctions in adult mouse lateral gastrocnemius. J Neurosci 10:1753–1761.

Wines MM, Letinsky MS (1988) Motor nerve terminal sprouting in formamide-treated inactive amphibian skeletal muscle. J Neurosci 8:3909–3919.

Xiao ZC, Deng L, Ko CP (1993) Identification of a synaptic extracellular matrix molecule from *Torpedo* electric organs. Soc Neurosci Abstr 19:700.